NASA Technical Memorandum 106682

Physical and Tribological Characteristics of Ion-Implanted Diamond Films

K. Miyoshi and S. Heidger
Lewis Research Center
Cleveland, Ohio

A.L. Korenyi-Both
Calspan Corporation
Fairview Park, Ohio

D.T. Jayne, P. Herrera-Fierro, and B. Shogrin
Case Western Reserve University
Cleveland, Ohio

P.J. Wilbur
Colorado State University
Fort Collins, Colorado

R.L.C. Wu
UES, Inc.
Dayton, Ohio

A. Garscadden and P.N. Barnes
Wright-Patterson Air Force Base
Dayton, Ohio

November 1994

National Aeronautics and
Space Administration

PHYSICAL AND TRIBOLOGICAL CHARACTERISTICS OF ION-IMPLANTED DIAMOND FILMS

K. Miyoshi and S. Heidger*
National Aeronautics and Space Administration
Lewis Research Center
Cleveland, Ohio 44135

A.L. Korenyi-Both
Calspan Corporation
Fairview Park, Ohio 44126

D.T. Jayne,** P. Herrera-Fierro,** and B. Shogrin**
Case Western Reserve University
Cleveland, Ohio 44106

P.J. Wilbur
Colorado State University
Fort Collins, Colorado 80523

R.L.C. Wu
UES, Inc.
Dayton, Ohio 45432

A. Garscadden and P.N. Barnes
Wright Laboratory
Wright-Patterson Air force Base
Dayton, Ohio 45433

SUMMARY

Unidirectional sliding friction experiments were conducted with a natural, polished diamond pin in contact with both as-deposited and carbon-ion-implanted diamond films in ultrahigh vacuum. Diamond films with a surface roughness ranging from 15- to 160-nm root-mean-square were deposited on silicon, silicon carbide, and silicon nitride by microwave-plasma-assisted chemical vapor deposition. The as-deposited diamond films were impacted with carbon ions at an accelerating energy of 60 keV and a current density of 50 $\mu A/cm^2$ for approximately 6 min, resulting in a dose of 1.2×10^{17} carbon ions/cm^2. The substrate temperatures during ion implantation did not exceed 200 °C.

The results indicate that the carbon ion implantation caused structural damage to the diamond lattice and produced a thin surface layer of amorphous, nondiamond carbon. The nondiamond carbon greatly decreased both friction and wear of the diamond films. The coefficients of friction for the carbon-ion-implanted, fine-grain diamond films were less than 0.1, factors of 20 to 30 lower than those for the as-deposited, fine-grain diamond films. The coefficients of friction for the carbon-ion-implanted, coarse-grain diamond films were approximately 0.35, a factor of 5 lower than those for the as-deposited, coarse-grain diamond films. The wear rates for the carbon-ion-implanted diamond films were on the order of 10^{-6} $mm^3/N \cdot m$, factors of 30 to 80 lower than that for the as-deposited diamond

---

*National Research Council—NASA Research Associate at Lewis Research Center.

**NASA Resident Research Associate at Lewis Research Center.

films, regardless of grain size. The friction of the carbon-ion-implanted diamond films was greatly reduced because the amorphous, nondiamond carbon, which had a low shear strength, was restricted to the surface layers (<0.1-μm thick) and because the underlying diamond materials retained their high hardness.

The primary mechanism of wear for both the as-deposited and carbon-ion-implanted diamond films was an adhesive interaction that caused small fragments to chip off the surface. The size (submicron to micron) and morphological characteristics of the wear debris particles were related to the wear rates. Much finer wear particles were generated on the surfaces of the carbon-ion-implanted diamond films than were generated on the surfaces of the as-deposited diamond films. In conclusion, the carbon-ion-implanted, fine-grain diamond films can be used effectively as wear-resistant, self-lubricating coatings for ceramics, such as silicon nitride and silicon carbide, in ultrahigh vacuum.

INTRODUCTION

Chemical-vapor-deposited diamond films have friction and wear properties similar to those of natural diamond in a variety of environments, such as humid air, dry nitrogen, and vacuum (refs. 1 and 2). It has been demonstrated that diamond films have low coefficients of friction μ (on the order of 0.01) and low wear rates ($<10^{-7}$ $mm^3/N \cdot m$) both in air and in dry nitrogen but that they have both high coefficients of friction ($\mu > 0.4$) and high wear rates (on the order of 10^{-4} $mm^3/N \cdot m$) in vacuum.

Similarly in vacuum, the coefficient of friction of diamond on diamond or diamond on metal can reach relatively high values ($\mu > 0.4$) compared with those observed in air and in dry nitrogen ($\mu < 0.1$ or 0.2) (refs. 1 to 8). For example, if the surfaces of the diamond and the metal are cleaned by argon ion bombardment, the coefficient of friction is high ($\mu > 0.4$, ref. 5). If the uncleaned surface of the diamond pin is allowed to repeatedly slide on the same track on the uncleaned surface of the diamond flat in vacuum, the relatively low initial coefficient of friction increases until it exceeds 0.4. Evidently, repeated sliding removes some contaminant surface film in vacuum (refs. 1, 3, and 4). Under these conditions, the adhesion between the sliding surfaces apparently plays a significant role in the friction process, and the surface roughness of diamond may not play an important role (ref. 1). Thus, it is clear that surface modifications that provide acceptable levels of friction and wear properties will be necessary before diamond films can be used for tribological applications in vacuum.

Previously, we found that carbon ion implantation at an accelerating energy of 160 keV and a dose of 6.7×10^{-7} carbon ions/cm^2 can form a thin layer of amorphous, nondiamond carbon. This nondiamond layer can reduce the coefficient of friction of diamond films in ultrahigh vacuum without sacrificing the low friction properties of diamond films in both air and dry nitrogen (refs. 9 and 10). The calculated penetration depth of the carbon ions was 198±27 nm. However, before the present study, neither the effect of carbon ion implantation on the wear behavior of diamond films nor the mechanisms of friction and wear had been described in detail.

The objectives of the present study were to

(1) Implant carbon ions into a variety of as-deposited, fine- and coarse-grain diamond films at an accelerating energy of 60 keV and a current density of 50 $\mu A/cm^2$ for 6 min, while keeping the substrate temperatures less than 200 °C to restrict the implanted carbon concentration to a surficial layer of 0.1 μm or less.

(2) Characterize the surface morphology and chemical composition of the films.

(3) Investigate the friction and wear behavior of these films in contact with a natural bulk diamond pin with a load of 0.49 N (mean hertzian contact pressure, 2.0 GPa) in an ultrahigh vacuum of 7×10^{-7} Pa at room temperature.

(4) Discuss the effects of carbon ion implantation and the mechanisms of the friction and wear of ion-implanted, fine-grain and coarse-grain diamond films in ultrahigh vacuum.

EXPERIMENT

Deposition of Diamond Films and Carbon Ion Implantation

The microwave-source plasma deposition system and the procedure used to deposit the diamond films are described in detail elsewhere (refs. 1 and 11). Briefly, in the deposition system, the microwave generator delivered up to 1 kW at 2.45 GHz to the plasma. The substrate was heated by a radiofrequency inductive heater. The processing gases and pressures were controlled with a flow controller and a pressure transducer. Ultrahigh purity (99.999%) H_2, ultrahigh purity (99.97%) CH_4, and extra dry (99.6%) O_2 were used to deposit the diamond films on the flat surfaces of silicon (Si), polycrystalline α-silicon carbide (SiC), and polycrystalline silicon nitride (Si_3N_4) substrates. The diamond nucleation density was enhanced by initially scratching the surfaces of the substrates with 0.5-μm diamond paste.

The deposition conditions strongly affected the crystalline structure and morphology of the diamond films. For example, figures 1(a) and (b) show that diamond crystallites (grains) in the as-deposited diamond films ranged from a ball-shaped morphology (fig. 1(a)) to a well-faceted morphology with pseudopentagonal symmetry (fig. 1(b)). Consequently, the deposition parameters controlling both the gas phase chemistry and surface chemistry were systematically investigated to produce the desired morphologies (refs. 1 and 11).

Carbon ions were implanted into the as-deposited diamond films by using a line-of-sight ion implanter at an accelerating energy of 60 keV and a current density of 50 $\mu A/cm^2$ for approximately 6 min, resulting in a dose of 1.2×10^{17} carbon ions/cm^2. Substrate temperatures during ion implantation did not exceed 200 °C. The carbon ions were implanted normal to the surfaces of the diamond films and penetrated to a calculated mean depth of 88 nm. Therefore, the dose yields a substantial implanted carbon concentration less than 0.1-μm thick in this ballistic layer.

The deposition and ion implantation conditions for the as-deposited and carbon-ion-implanted diamond films used in the friction and wear experiments are listed in tables I and II.

Diamond Films Characterization

A variety of techniques were used to characterize the as-deposited and the carbon-ion-implanted diamond films: scanning and transmission electron microscopy (SEM and TEM) to determine surface morphology and measure grain sizes; surface profilometry to measure the surface roughness by using a diamond stylus tip (12.5 μm in radius) that traversed at a load of 0.4 mN (40 mg) over a scanning length of 2 mm; Raman spectroscopy (table III) and Fourier transform infrared spectroscopy (FTIR) to characterize diamond quality and structure; x-ray photoelectron spectroscopy (XPS) to characterize surface chemistry; Rutherford backscattering spectroscopy (RBS) to identify impurities (if any) in the films and to determine carbon and impurity concentrations; proton recoil detection (PRD) to measure the hydrogen concentration; and x-ray diffraction to determine the crystal orientation of the as-deposited diamond films.

Friction and Wear Experiment

Unidirectionally rotating, multipass sliding friction experiments were conducted with diamond films in contact with a natural bulk diamond pin (ref. 1). The radius of curvature at the apex of the diamond pin was approximately 1.3 mm, and the (112) plane of the diamond pin was oriented such that it was nearly parallel to the sliding interface. All sliding was conducted in the <111> direction of the diamond pin. Before each experiment, the diamond pin was repolished with diamond powder (1 μm in diameter) and was ultrasonically rinsed in an ethanol bath. Multipass sliding friction

experiments were conducted with a load of 0.49 N (mean hertzian contact pressure, approximately 2 GPa) in an ultrahigh vacuum of $7x10^{-7}$ Pa at room temperature (table IV). The friction force was continuously monitored during the friction experiments. Wear volumes of the diamond films were obtained by measuring the cross-sectional area from stylus tracings across the wear tracks, at a minimum of eight locations in each track. Then, the average cross-sectional area of the wear track was multiplied by the wear track length. The wear rate is defined as the volume of material removed in unit applied load and in unit sliding distance and is expressed as cubic millimeters per newton-meter.

RESULTS AND DISCUSSION

Diamond Films and Their Surfaces

Surface morphology and roughness.—The as-deposited diamond films used in the friction and wear experiments were separated into two morphological types: smooth, fine-grain diamond films and rough, coarse-grain diamond films.

In the fine-grain diamond films, the crystallites had a granulated or spherulitic morphology. The surfaces contained spherical asperities of different sizes (e.g., fig. 2). The surface roughness and grain size of the as-deposited, fine-grain diamond films ranged from 6- to 37-nm root-mean-square (rms) and from 20 to 100 nm, respectively (table I).

In the coarse-grain diamond films, the crystallites had a triangular-faceted morphology typical of diamond. The surfaces contained cubic and octahedral asperities and a rough morphology (e.g., fig. 3). The surface roughness and grain size of the as-deposited, coarse-grain diamond films ranged from 36 to 160 nm rms and from 1000 to 3300 nm, respectively (table I).

No significant changes in surface morphology and surface roughness resulted from the carbon ion implantation (figs. 2 and 3, tables I and II). The surface features of the carbon-ion-implanted, fine- and coarse-grain diamond films were almost the same as those of the as-deposited, fine- and coarse-grain diamond films. The only morphological effect of the carbon ion implantation was the rounding of edges (figs. 2 and 3). Carbon ion implantation on the fine-grain diamond films with a granulated or spherulitic morphology produced surfaces with somewhat blunt, rounded grains (fig. 2). Likewise, the edges of the grains in the coarse-grain diamond films were somewhat rounded as a result of the carbon ion implantation (fig. 3). Edge shape could have a strong influence on the wear of counterfacing material, and rounded edges may reduce wear.

Bulk and surface chemistry.—RBS of the as-deposited diamond films revealed that they consisted of carbon and some elements from the substrate material, such as Si (refs. 1 and 11). From the PRD data, the hydrogen concentration was estimated to be 2.5 at.% in the as-deposited, fine-grain diamond films and less than 1 at.% in the as-deposited, coarse-grain diamond films (refs. 1 and 11).

Figures 4(a) and (b) present a Raman spectrum of type IIa, single-crystal (111) diamond as a reference and a Raman spectrum of an as-deposited, coarse-grain diamond film, respectively. In figure 4(a), the presence of diamond bonding is unambiguous and clear in the Raman spectrum of the single-crystal diamond. Single-crystal diamond is identified by a single sharp Raman peak at a wavenumber of 1332 cm^{-1}.

In figure 4(b), the Raman spectrum of a coarse-grain diamond film is deconvolved. When the Raman spectra of both the as-deposited, fine- and coarse-grain diamond films are deconvolved, three bands characteristic of chemical-vapor-deposited (CVD) diamond films are revealed: (1) a sharp band centered near 1330 cm^{-1}, (2) a broad band centered in the 1500- to 1530-cm^{-1} range, and (3) an even broader band centered near 1320 cm^{-1}. The sharp band centered near 1330 cm^{-1} is characteristic of the sp^3 bonding of diamond. The two broad, overlapping bands centered near 1500 to 1530 cm^{-1} and near 1320 cm^{-1} are characteristic of the nondiamond form of carbon and are referred to as the G band and D band, respectively. The Raman shifts referred to as the G band are attributed to the sp^2-bonded

carbon, whereas the Raman shifts referred to as the D band are attributed to the disorder of the nondiamond carbon present in the films (refs. 12 to 14).

Because the Raman technique is approximately 50 times more sensitive to the sp^2-bonded form of carbon than it is to the diamond form, the as-deposited diamond films actually contain much more of the diamond form of carbon than may be inferred from the spectra (figs. 5, 6, and 7). The frequencies, half-widths, intensity ratios, and slopes of the photoluminescence backgrounds for the Raman spectra of both as-deposited and carbon-ion-implanted diamond films are listed in table V. As indicated by the relative intensities of the diamond band in comparison to the nondiamond carbon bands, the as-deposited, fine-grain diamond films contained considerably more nondiamond carbon than the coarse-grain diamond films. Both the frequency and half-width of the diamond band were related to the grain size of the diamond films. For films with smaller grain sizes, the diamond peak was broader and located at a higher phonon frequency. In addition, micro-Raman spectroscopy shows the presence of Si-O in the fine-grain diamond film on the Si (100) substrate, whereas hexagonal α-SiC is present in the coarse-grain diamond film deposited on the Si_3N_4 substrate.

In figures 5, 6, and 7, the very broad band with a peak near 1500 to 1530 cm^{-1} and a shoulder near 1320 cm^{-1}, indicative of the amorphous, nondiamond form of carbon, is the prominent feature in the Raman spectra. The characteristic diamond peak is absent from the micro-Raman spectra of the carbon-ion-implanted diamond films. However, after carbon ion implantation no significant change in the surface morphology was observed by SEM or TEM. Hence, the difference between the Raman spectra of the as-deposited and carbon-ion-implanted diamond films can be interpreted as twofold: (1) the intensity of the Raman bands from the nondiamond carbon increased, and (2) the intensity of the diamond peak decreased to the extent that the diamond peak could not be resolved from the much larger nondiamond carbon bands in the time that the spectra were collected.

Because the depth sensitivity of micro-Raman spectroscopy is one micrometer or less, the significant decrease in the intensity of the diamond peak observed after carbon ion implantation is evidence of both the formation of a nondiamond surface layer on top of the diamond films and of structural damage and distortion from the cubic diamond structure. Furthermore, the increased frequency shift of the G band and the D band after carbon ion implantation indicates that the nondiamond carbon layer contains more sp^2-bonded carbon than does the nondiamond carbon present in the as-deposited diamond films. These results are consistent with those from the Raman analysis conducted in the previous study. Ion implantation of carbon (at an accelerating energy of 160 keV and a dose of 6.7×10^{17} carbon ions/cm^2) and of nitrogen (at an accelerating energy of 35 keV and a dose of 5×10^{16} nitrogen ions/cm^2) caused structural surface damage to both the fine-grain and coarse-grain diamond films, as well as to the polished diamond films. The ion implantation processes also produced a thin layer of nondiamond carbon (refs. 9 and 10).

FTIR of both the as-deposited and carbon-ion-implanted diamond films showed absorbance only in the 600 to 1500 cm^{-1} range. Only very weak absorbance was observed in the C-H stretch region for either the as-deposited or the carbon-ion-implanted diamond films. This is consistent with the low hydrogen concentration determined by PRD analysis. From the FTIR spectra, the composition of the sampling region appeared quite uniform. However, absorbances from both the films and the substrates were observed in the FTIR spectra. Figure 8 shows the FTIR spectrum resulting when the spectrum of an as-deposited diamond film is subtracted from the spectrum of the carbon-ion-implanted diamond film. The FTIR spectrum of the carbon-ion-implanted diamond film has a much larger peak around 832 cm^{-1} than the as-deposited diamond film has. This absorption band, which seems to vary in intensity across the implanted film, has been attributed to aromatic ring breathing. This attribution is consistent with the Raman spectra interpretation that carbon-ion-implanted films have more sp^2 bonding than the as-deposited diamond films have.

XPS spectra of the surfaces of coarse- and fine-grain, as-deposited and carbon-ion-implanted diamond films are shown in figure 9. All four surfaces contained oxygen, with C/O ratios ranging between 8 and 12. Several atomic percent of nitrogen and silicon were detected in the surfaces of both the as-deposited and carbon-ion-implanted, coarse-grain diamond films. The plasmon loss structure for

the C 1s peak of as-deposited and carbon-ion-implanted diamond films indicates that carbon ion implantation decreases the sp^3/sp^2 ratio of carbon bonds at the surface (ref. 15). Furthermore, the carbon-ion-implanted diamond films were more conductive than the as-deposited diamond films during analysis, indicating that carbon ion implantation alters the normally insulating diamond surface to a conductive carbon surface.

Crystal structure.—X-ray diffraction data revealed that although most of the crystallites in the as-deposited, fine-grain diamond films were oriented along (110) planes, those of the as-deposited, coarse-grain diamond films were oriented along (111) planes (refs. 1 and 11). The well-formed triangular facets of the coarse-grain diamond films observed in SEM photomicrographs (see fig. 3) confirm the (111) orientation.

Friction and Wear Characteristics

Coefficient of friction.—Figures 10 and 11 show coefficients of friction obtained in ultrahigh vacuum for both as-deposited and carbon-ion-implanted diamond films on Si, SiC, and Si_3N_4 plotted as functions of the number of revolutions.

Fine-grain diamond films: Figure 10 shows the coefficients of friction for fine-grain diamond films. The median coefficients of friction of the as-deposited, fine-grain diamond films on Si, SiC, and Si_3N_4 between 20 and 300 revolutions were 1.3, 1.6, and 1.2, respectively. The median coefficients of friction obtained for the carbon-ion-implanted diamond films on Si, SiC, and Si_3N_4 for 1500 revolutions were 0.05, 0.07, and 0.06, respectively. Beyond 1500 revolutions, the median coefficients of friction of the carbon-ion-implanted diamond films gradually increased to a maximum value of approximately 0.35 at 5000 revolutions, regardless of the substrate.

Coarse-grain diamond films: Figure 11 shows the coefficients of friction for coarse-grain diamond films. Between 20 and 300 revolutions, the median coefficients of friction of the as-deposited, coarse-grain diamond films on Si, SiC, and Si_3N_4 were 1.4, 1.6, and 1.5, respectively. The carbon-ion-implanted, coarse-grain diamond films had median coefficients of friction which were a factor of 4 to 5 lower than those obtained for the as-deposited diamond films. However, the median coefficients of friction of the carbon-ion-implanted diamond films were still relatively high, approximately 0.35 at 10 000 revolutions, regardless of the substrate.

Wear surface and debris.—SEM analysis of the wear scars produced on the diamond pin by the sliding action revealed that the wear surface was generally smooth, regardless of the counterfacing material (fine-grain and coarse-grain diamond films). Figure 12(a) shows an example of a diamond pin wear scar. Thin, smeared patches of wear debris generally covered the smooth wear scars. Most of the loose and smeared wear debris accumulated outside the wear scars. The wear debris smeared out into tongues pointing away from the sliding direction.

The diamond pin grooved the surfaces of both fine- and coarse-grain diamond films in ultrahigh vacuum. As an example, the SEM and the profilometer record of a wear track produced on a diamond film are presented in figures 12(b) and (c), respectively. The surfaces of wear tracks were generally smooth as were the surfaces of the wear scars. Likewise, most of the loose wear debris had accumulated on the outside of the wear tracks. Smeared patches of wear debris were present on a relatively small fraction of the overall area of the wear tracks.

Fine-grain diamond films: Figures 13(a) and (b) present examples of a wear track and wear debris, respectively, produced on the as-deposited, fine-grain diamond films by sliding action. The SEM photomicrographs generally revealed two different areas: (1) light areas, which are identified as original surface features of the as-deposited, fine-grain diamond films, and (2) dark areas, which are identified as the wear surfaces on the tips of the asperities. The wear debris deposited on the outside of the smooth wear tracks generally consisted of individual, fine (submicron) wear debris particles and agglomerated, pasty wear debris.

Figures 14(a) and (b) present examples of a wear track and wear debris, respectively, produced on the carbon-ion-implanted, fine-grain diamond films by sliding action. The sliding action generated fine (submicron) wear debris particles and agglomerated, pasty wear debris particles, which were much finer than those on the as-deposited diamond films. Smeared tongues of thin, layered, agglomerated wear debris particles were also present.

Coarse-grain diamond films: Figure 15 presents examples of wear tracks produced by sliding action on the as-deposited, coarse-grain diamond films. Similar to the fine-grain diamond films, the SEM photomicrographs generally revealed two different areas: (1) light areas, which are identified as the original surface features of the as-deposited, coarse-grain diamond films, and (2) dark areas, which are identified as both the wear surfaces on the tips of the high asperities and regions where valleys and lower asperities were filled with smeared, pasty wear debris. The wear debris deposited on the wear tracks and their surroundings generally contained individual, fine (submicron) debris particles and agglomerated, pasty debris.

With the carbon-ion-implanted, coarse-grain diamond films, SEM observations revealed that wear had occurred on the tips of the high asperities (figs. 16(a) and (b)). The sliding action and wear generated individual, fine (submicron) debris particles and smeared, agglomerated pasty particles on and around the asperities. Large amounts of wear debris were also found on the wear tracks and their surroundings (figs. 16(b) and (c)). The wear debris particles generated on the carbon-ion-implanted, coarse-grain diamond films were similar to those generated on the carbon-ion-implanted, fine-grain diamond films.

Wear rate.—Figure 17 presents the average wear rates of the as-deposited and carbon-ion-implanted diamond films in ultrahigh vacuum. The average wear rates and their standard deviations for the as-deposited and carbon-ion-implanted diamond films on Si, SiC, and Si_3N_4 substrates are shown in table VI. The wear rates for the carbon-ion-implanted diamond films were much lower, by factors of 30 to 80, than for the as-deposited diamond films.

Discussion

Carbon ion implantation effects.—It has been recognized that bombardment of diamond by ions can cause structural damage—an increase in volume with a corresponding increase in interplanar spacings and the production of amorphous, nondiamond carbon layers (refs. 16 to 19).

The carbon ion implantation process (at an accelerating energy of 60 keV and a dose of 1.2×10^{17} carbon ions/cm^2) changes the surface chemistry of the CVD, fine- and coarse-grain diamond films and structurally damages the diamond lattice. Consequently, carbon ion implantation produces a thin layer of amorphous, nondiamond carbon in the near surface region of diamond films (figs. 5 to 7). This effect is consistent with that of carbon ion implantation at an accelerating energy of 160 keV and a dose of 6.7×10^{17} carbon ions/cm^2 and of nitrogen ion implantation at an accelerating energy of 35 keV and a dose of 5×10^{16} nitrogen ions/cm^2 (from the previous study, refs. 9 and 10).

The surface roughness for both fine- and coarse-grain diamond films increased after carbon ion implantation at the high accelerating energy of 160 keV (ref. 9). However, neither carbon ion implantation at the relatively low accelerating energy of 60 keV used in the present study nor nitrogen ion implantation at the low accelerating energy of 35 keV appreciably influenced the surface roughness or morphology of the fine-grain, coarse-grain, or polished diamond films.

At the low accelerating energy of 60 keV and a dose of 1.2×10^{17} carbon ions/cm^2, the effects of carbon ion implantation on friction and wear behavior in ultrahigh vacuum were twofold: (1) a reduction in the coefficient of friction and (2) an increase in the wear resistance. The median coefficients of friction obtained for the carbon-ion-implanted, fine-grain diamond films were less than 0.1, factors of 20 to 30 lower than those obtained for the as-deposited diamond films. The average wear rates for the carbon-ion-implanted, fine-grain diamond films were on the order of 10^{-6} mm^3/N·m, factors of 30 to 60 lower than those obtained for the as-deposited, fine-grain diamond films.

Likewise, the median coefficients of friction obtained for the carbon-ion-implanted, coarse-grain diamond films were approximately 0.35, a factor of 5 lower than those obtained for the as-deposited diamond films. The average wear rates for the carbon-ion-implanted, coarse-grain diamond films were on the order of 10^{-6} $mm^3/N \cdot m$, factors of 30 to 80 lower than those obtained for the as-deposited, coarse-grain diamond films.

Mechanisms of friction.—The high coefficients of friction ($\mu > 1.0$) for the as-deposited, fine- and coarse-grain diamond films in contact with a diamond pin in ultrahigh vacuum arise primarily from the adhesion between the sliding surfaces (ref. 1). The presence of dangling bonds on the surfaces of the diamond films may play a significant role in the high friction process in vacuum (refs. 4 and 6).

Fine-grain diamond films: Because the surface is smooth and the asperities are round, if we neglect the plowing term the friction arising between the fine-grain diamond film and the diamond pin in ultrahigh vacuum can be described by the equation $\mu = sA/W$, where μ is the coefficient of friction, s is the shear strength of junctions, A is the true contact area, and W is the normal contact load (refs. 20 and 21). In the case of the as-deposited diamond films, the area of contact is small because of the high elastic modulus and high hardness of diamond, but s is correspondingly high. For this reason, the coefficient of friction of the as-deposited diamond films is high ($\mu > 1.0$).

In the case of the carbon-ion-implanted diamond films, because the nondiamond carbon surface layer formed is thin (<0.1 μm) the contact load is largely supported by the hard diamond films. Consequently, the true area of contact is again small. However, the nondiamond carbon has low shear strength. The combination of the low shear strength of the thin, nondiamond carbon surface layer and the small contact area resulting from the high elastic modulus of diamond gives rise to low coefficients of friction ($\mu < 0.1$) for the carbon-ion-implanted, fine-grain diamond films.

When the nondiamond carbon surface layer was removed from the diamond film during repeated sliding action, the coefficient of friction increased. Thus, the thin, nondiamond carbon surface layer produced by carbon ion implantation provides lubrication in ultrahigh vacuum.

Coarse-grain diamond films: Even though the surface asperities of the as-deposited, coarse-grain diamond films have sharp tips, adhesion between the sliding surfaces of the diamond pin and diamond films still played the most significant role in friction in ultrahigh vacuum; plowing due to the interaction of the sharp asperities with the diamond pin was insignificant. As reported earlier, the surface roughness of the as-deposited diamond films did not have much influence on the coefficient of friction of diamond films in ultrahigh vacuum (ref. 1).

On the other hand, the coefficients of friction of the carbon-ion-implanted, coarse-grain diamond films, which were approximately 0.35, are an order of magnitude higher than those of the carbon-ion-implanted, fine-grain diamond films. Even in ultrahigh vacuum, surface roughness affects the coefficients of friction of the carbon-ion-implanted diamond films. This effect is similar to that on the friction behavior of as-deposited diamond films in laboratory air and in dry nitrogen environments (ref. 1). The two most significant factors influencing the coefficients of friction of the carbon-ion-implanted, coarse-grain diamond films are (1) plowing between the sharp asperities and the diamond pin and (2) adhesion at the frictional junction, which is relatively low because the nondiamond carbon surface layer produced by carbon ion implantation has low shear strength.

Mechanisms of wear.—Debris generated by sliding action provide a useful history of the wear process (ref. 22). In addition to the quantity and size of the wear debris particles, much useful information can be obtained from microscopic observation of their nature and shape (refs. 22 and 23).

SEM observations indicate that the mechanism of wear for the as-deposited and carbon-ion-implanted diamond films was an adhesive interaction that caused small fragments to chip off the surface of both the as-deposited and carbon-ion-implanted diamond films. Wear debris particles (submicron to micron in size) were observed on the surfaces of both the diamond pin and the diamond film. Much finer particles were generated on the surfaces of the carbon-ion-implanted diamond films than on the surfaces of the as-deposited diamond films. The generation of finer wear debris particles from the surfaces of carbon-ion-implanted diamond films primarily resulted from the wear and

removal of amorphous, nondiamond carbon by sliding. The size differences of the wear particles contributed to their respective wear rates. The wear rates of the carbon-ion-implanted diamond films (on the order of 10^{-6} $mm^3/N \cdot m$) are considerably lower than those of the as-deposited diamond films (on the order of 10^{-4} $mm^3/N \cdot m$).

SUMMARY OF RESULTS

Carbon ion implantation at an accelerating energy of 60 keV and a dose of 1.2×10^{17} carbon ions/cm^2 changes the surface chemistry of microwave-plasma vapor deposited, fine- and coarse-grain diamond films and causes structural damage to the diamond lattice.

The coefficients of friction for the carbon-ion-implanted, fine-grain diamond films were less than 0.1, factors of 20 to 30 lower than those for the as-deposited diamond films. The coefficients of friction for the carbon-ion-implanted, coarse-grain diamond films were approximately 0.35, a factor 5 lower than those for the as-deposited diamond films.

The wear rates for the carbon-ion-implanted diamond films were on the order of 10^{-6} $mm^3/N \cdot m$, factors of 30 to 80 lower than that for the as-deposited diamond films (on the order of 10^{-4} $mm^3/N \cdot m$), regardless of diamond grain size. The characteristics of wear debris particles (submicron to micron in size) were related to the wear rates. Much finer particles were generated on the surfaces of the carbon-ion-implanted diamond films than on the surfaces of the as-deposited diamond films.

CONCLUSIONS

From the results of characterization and sliding friction experiments on as-deposited and carbon-ion-implanted diamond films in ultrahigh vacuum, the following conclusions were drawn.

1. Carbon ion implantation produces a thin layer of amorphous, nondiamond carbon in the near surface region of diamond films.
2. The presence of an amorphous, nondiamond carbon layer produced by carbon ion implantation at 60 keV greatly decreased both the friction and wear of microwave-plasma deposited diamond films.
3. The friction of carbon-ion-implanted diamond films was greatly reduced because the amorphous, nondiamond carbon, which possesses low shear strength, was restricted to the surface layers (<0.1-μm thick) and because the underlying diamond films retained their high hardness.
4. The mechanism of wear for the as-deposited and carbon-ion-implanted diamond films was primarily an adhesive interaction that caused small fragments to chip off the surfaces.
5. The carbon-ion-implanted, fine-grain diamond films can be effectively used as wear-resistant, self-lubricating coatings for ceramics, such as Si_3N_4 and SiC, in ultrahigh vacuum.

ACKNOWLEDGMENTS

This work was supported by the Vehicle Propulsion Directorate of the U.S. Army Research Laboratory (task YOA 0304; RTOP-505-62-OR). The authors thank R.C. Bill for his helpful discussions. The authors are also grateful to A.K. Sarkar of University of Dayton Research Institute for the x-ray diffraction analyses.

REFERENCES

1. Miyoshi, K.; et al.: Friction and Wear of Plasma-Deposited Diamond Films. J. Appl. Phys., vol. 74, no. 7, Oct. 1993, pp. 4446-4454.

2. Miyoshi, K.; Wu, R.L.C.; and Garscadden, A.: Friction and Wear of Diamond and Diamondlike Carbon Coatings. Surf. Coat. Technol., vol. 54/55, 1992, pp. 428-434.

3. Bowden, F.P.; and Hanwell, A.E.: The Friction of Clean Crystal Surfaces. Proc. R. Soc. London Ser. A, vol. 295, 1966, pp. 233-243.

4. Tabor, D.: Properties of Diamond. J.E. Field, ed., Academic Press, New York, 1979, pp. 325-350.

5. Miyoshi, K.; and Buckley, D.H.: Adhesion and Friction of Single-Crystal Diamond in Contact With Transition Metals. Appl. Surf. Sci., vol. 6, 1980, pp. 161-172.

6. Gardos, M.N.; and Ravi, K.V.: Tribological Behavior of CVD Diamond Films. Electrochem. Soc. Proc., vol. 89, 1989, pp. 475-493.

7. Hayward, I.P.: Friction and Wear Properties of Diamonds and Diamond Coatings. Surf. Coat. Technol., vol. 49, 1991, pp. 554-559.

8. Dugger, M.T.; Peebles, D.E.; and Pope, L.E.: Surface Science Investigations in Tribology. Y.-W. Chung, A.M. Homola, and G.B. Street, eds., American Chemical Society, Washington, D.C., 1992, pp. 72-102.

9. Wu, R.L.C.; et al.: Ion-Implanted Diamond Films and Their Tribological Properties. Surf. Coat. Technol., vol. 62, 1993, pp. 589-594.

10. Wu, R.L.C.; et al.: Tribological and Physical Properties of Ion-Implanted Diamond Films. Diamond Films and Technology, vol. 3, no. 1, 1993, pp. 17-29.

11. Wu, R.L.C.; et al.: Synthesis and Characterization of Fine-Grain Diamond Films. J. Appl. Phys., vol. 72, no. 1, Jul. 1992, pp. 110-116.

12. Chang, J.J.; et al.: Effects of Oxygen and Pressure on Diamond Synthesis in a Magnetoactive Microwave Discharge. J. Appl. Phys., vol. 71, no. 6, Mar. 1992, pp. 2918-2923.

13. Kobayashi, K.; et al.: Synthesis of Diamonds by Use of Microwave Plasma Chemical Vapor Deposition: Morphology and Growth of Diamond Film. Phys. Rev. B, vol. 38, no. 6, Aug. 1988, pp. 4067-4084.

14. Pierson, H.O.: Handbook of Carbon, Graphite, Diamond and Fullerenes. Noyes Publications, Park Ridge, New Jersey, 1993, pp. 244-277.

15. Schmieg, S.J.; and Belton, D.N.: Polycrystalline Diamond Film on Si (100) by XPS. Sur. Sci. Spectra., vol. 1, no. 4, 1993, pp. 331-332.

16. Nikolaenko, V.A.; Gordeev, V.G.; and Zaytev, A.M.: Bombardment of Diamond With Carbon Ions. Radiat. Eff., vol. 83, 1984, p. 11-16.

17. Vance, E.R.: X-Ray Study of Neutron-Irradiated Diamonds. J. Phys. C, vol. 4, no. 3, Mar. 1971, pp. 257-262.

18. Vavilov, V.S.: Ion Implantation Into Diamond. Radiat. Eff., vol. 37, 1978, p. 229-236.

19. Maby, E.W.; Magee, C.W.; and Morewood, J.H.: Volume Expansion of Ion-Implanted Diamond. Appl. Phys. Lett., vol. 39, no. 2, Jul. 1981, pp. 157-158.

20. Bowden, F.P.; and Tabor, D.: The Friction and Lubrication of Solids. Clarendon Press, Oxford, 1958, pp. 52-86.

21. Roberts, E.W.: Ultralow Friction Films of MoS_2 for Space Applications. Thin Solid Films, vol. 181, 1989, pp. 461-473.

22. Barwell, F.T.: Handbook of Lubrication, Vol. 2, E.R. Booser, ed., 1984, pp. 163-184.

23. Rabinowicz, E.: Handbook of Lubrication, Vol. 2, E.R. Booser, ed., 1984, pp. 201-208.

TABLE I.—DEPOSITION CONDITIONS FOR DIAMOND FILMS

Substrate[a]	Deposition										
	Gaseous flow rate, cm^3/min			Pressure		Micro-wave power, kW	Deposition temperature, °C	Deposition time, h	Thick-ness, nm	Grain size, nm	Surface rough-ness, nm rms
	CH_4	H_2	O_2	Pa	Torr						
Si (100)	4	395	1	665	5	0.5	860±20	10.5	1000	20 to 100	6±5
α-SiC	4	395	1	665	5	0.5	860±20	21	1000	22 to 100	37±9
Si_3N_4	4	395	1	665	5	0.5	860±20	21	800	22 to 100	21±3
Si (100)	3.5	500	0	5320	40	1	1015±50	14	4200	1100	47±10
α-SiC	3.5	500	0	5320	40	1	965±50	22	8000	1500	36±15
α-SiC	3.5	500	0	5320	40	1	1015±50	14	5000	3300	160±19
Si_3N_4	3.5	500	0	5320	40	1	965±50	22	7000	1000	63±5

[a]Scratched with 0.5-μm diamond paste.

TABLE II.—ION IMPLANTATION CONDITIONS FOR DIAMOND FILMS

[Energy, 60 keV; dose, $1.2x10^{17}$ carbon ions/cm^2; dose rate, 50 μA/cm^2; time, 6 min.]

Substrate	C^+ Ion implantation	
	Temperature, °C	Surface roughness, nm rms
Si (100)	<100	14±13
α-SiC	<125	30±5
Si_3N_4	<180	24±4
Si (100)	<100	49±9
α-SiC	<195	39±9
α-SiC	----	----
Si_3N_4	<115	51±6

TABLE III.—RAMAN ANALYSIS

[Micro-Raman Spectrometer using the 514.53-nm green line from an argon-ion laser.]

Laser power, mW	<10
Microscope magnification	x50
Confocal slit, μm	25
Scan range, cm^{-1}	600 to 1900
Collection time, sec	10
Resolution, cm^{-1}	1

TABLE IV.—CONDITIONS OF FRICTION AND WEAR EXPERIMENT

Motion	Rotating
Radius of curvature at apex of diamond pin, mm	1.3
Load, N	0.49
Initial average Hertian contact pressure, GPa	2.0
Disk rotating speed, rpm	20
Track diameter, mm	7 to 13
Sliding velocity, mm/sec	7 to 10
Vacuum pressure, Pa (Torr)	10^{-7} (10^{-9})
Temperature, °C	23

TABLE V.—MICROWAVE CHEMICAL-VAPOR-DEPOSITED DIAMOND RAMAN SPECTRA
[Excitation, 514.5 nm.]

Substrate	Grain size, nm	As-deposited diamond						Carbon-ion-implanted diamond				
		Raman bands			Intensity ratio		PL slope, cm	Raman bands			Intensity ratio, A_d/A_g	PL slope, cm
		Band	Frequency, cm^{-1}	HWHM, cm^{-1}	A_{di}/A_{nd}	A_d/A_g		Band	Frequency, cm^{-1}	HWHM, cm^{-1}		
Si (100)	20 to 100	Di	1330	12.3	0.008	1.04	7.78	D_i	----	-----	0.82	0.41
		D	1361	131.3				D	1368	185.3		
		G	1537	92.4				G	1536	107.5		
Si_3N_4	1000	Di	1328	8.44	0.089	0.87	18.04	D_i	----	-----	0.95	0.86
		D	1361	129.6				D	1365	197.0		
		G	1538	93.8				G	1537	102.8		
α-SiC	1500	Di	1327	7.94	0.130	0.70	24.09	D_i	----	-----	1.60	1.05
		D	1353	113.4				D	1394	214.8		
		G	1528	92.5				G	1544	97.5		

Di Diamond band
D Disorder band
G Graphite band
A_{di}/A_{nd} Ratio of area under the diamond band to the area under the nondiamond carbon bands
A_d/A_g Ratio of the area under the disorder band to the area under the graphite band
HWHM Half width at half maximum of Raman band
PL slope Slope of the photoluminescence background

TABLE VI.—WEAR RATES OF AS-DEPOSITED AND ION-IMPLANTED DIAMOND FILMS

Substrate	Wear rate, $10^{-6}mm^3/N \cdot m$			
	As-deposited films		Ion-implanted films	
	Fine grain	Coarse grain	Fine grain	Coarse grain
Si	122±60	189±98	1.9±0.86	5.4±1.5
SiC	130±73	340±145	2.2±1.2	4.4±1.3
Si_3N_4	87±55	170±82	2.6±0.56	5.2±1.2

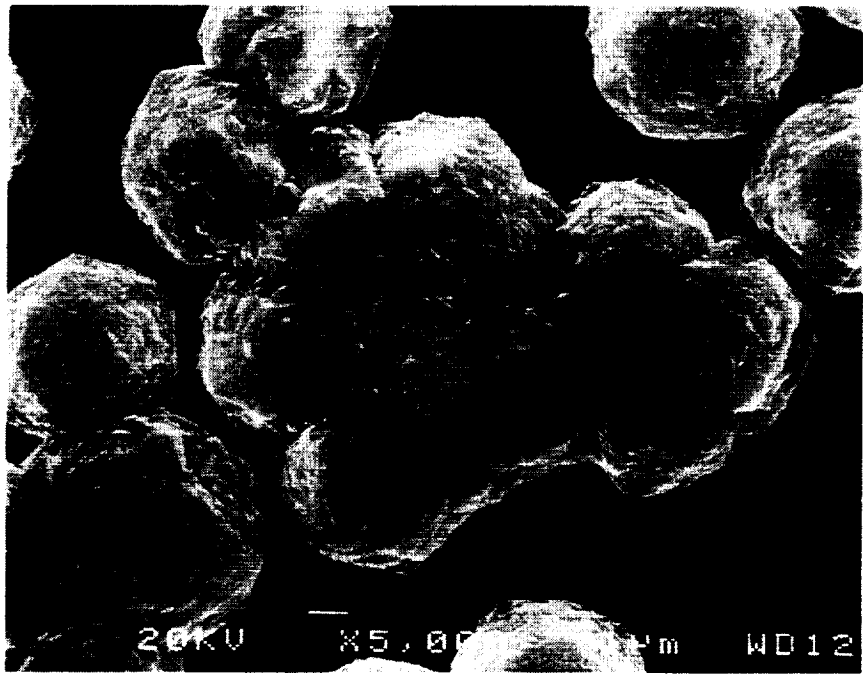

(a) 1 μm

(b) 1 μm

Figure 1.—Growth shape of diamond crystallites. (a) Ball-shaped morphology. (b) Faceted morphology.

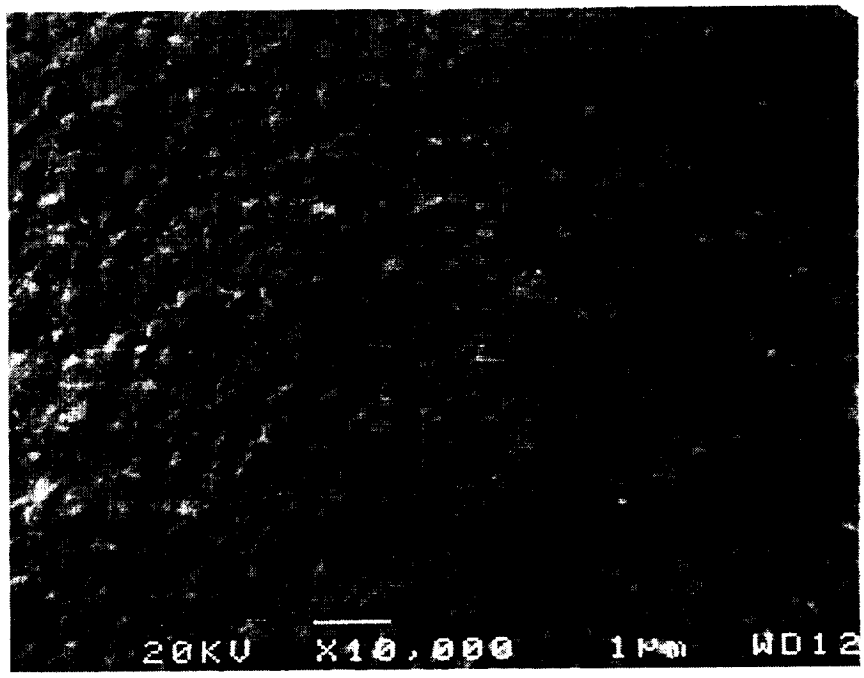

(a)

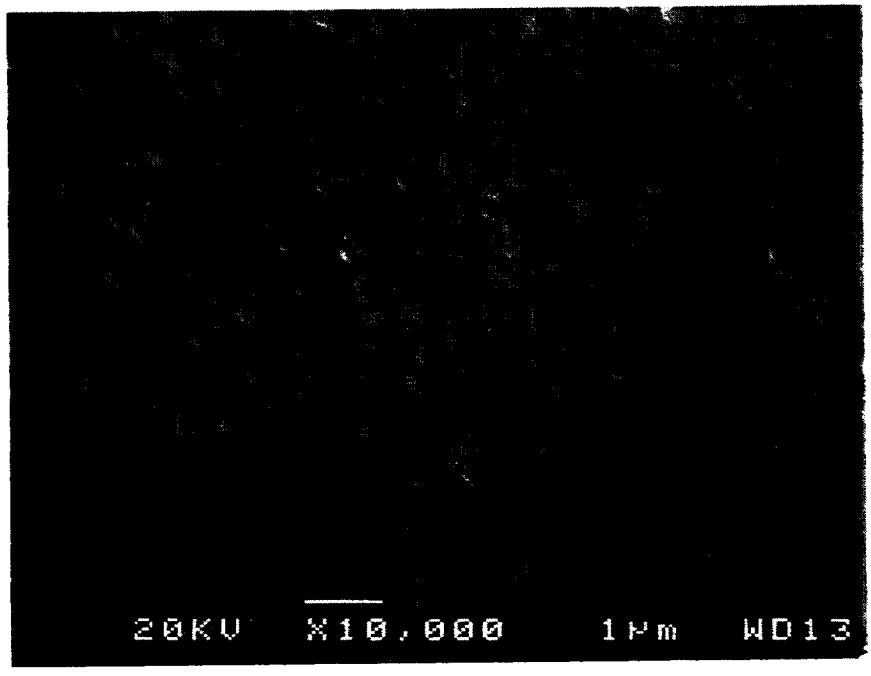

(b)

Figure 2.—Scanning electron micrographs of fine-grain diamond films. (a) As-deposited film on a Si_3N_4 substrate. (b) Carbon-ion-implanted film on a Si_3N_4 substrate.

(a) 1 μm

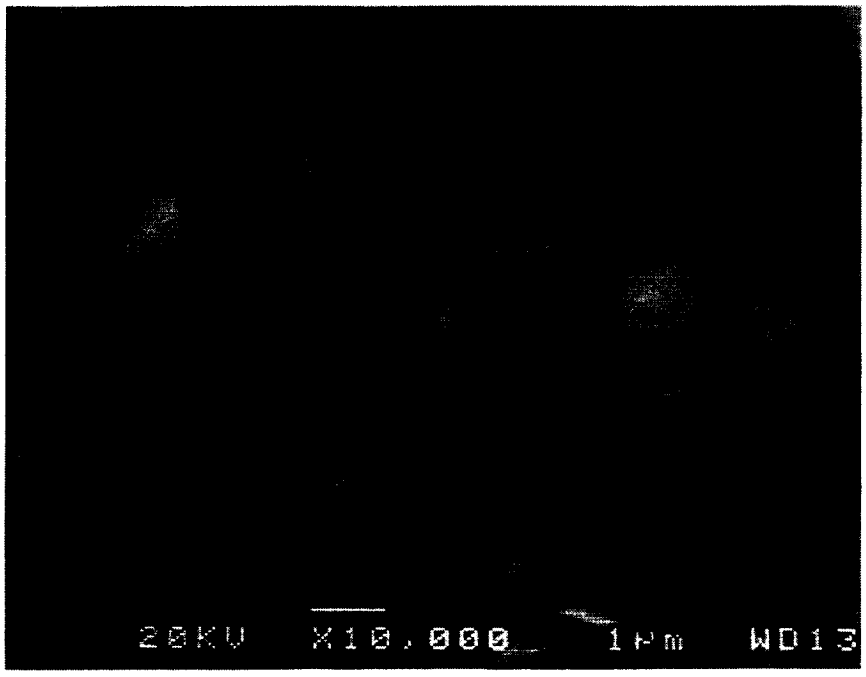

(b) 1 μm

Figure 3.—Scanning electron micrographs of coarse-grain diamond films. (a) As-deposited film on a Si_3N_4 substrate. (b) Carbon-ion-implanted film on a Si_3N_4 substrate.

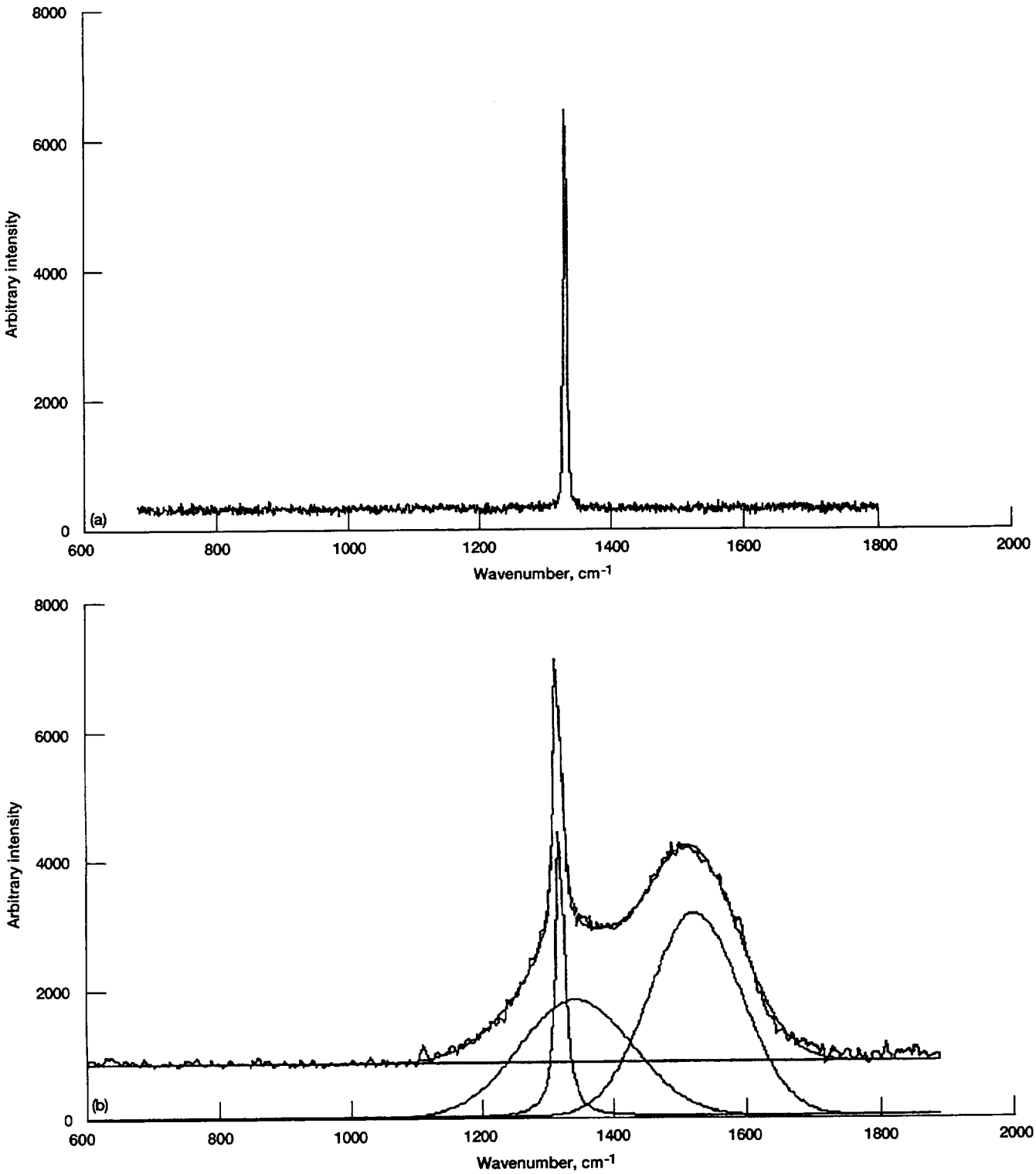

Figure 4.—Raman spectra of a natural diamond and an as-deposited, coarse-grain diamond film. (a) Natural diamond. (b) Deconvolution of Raman bands from as-deposited, coarse-grain diamond film on SiC.

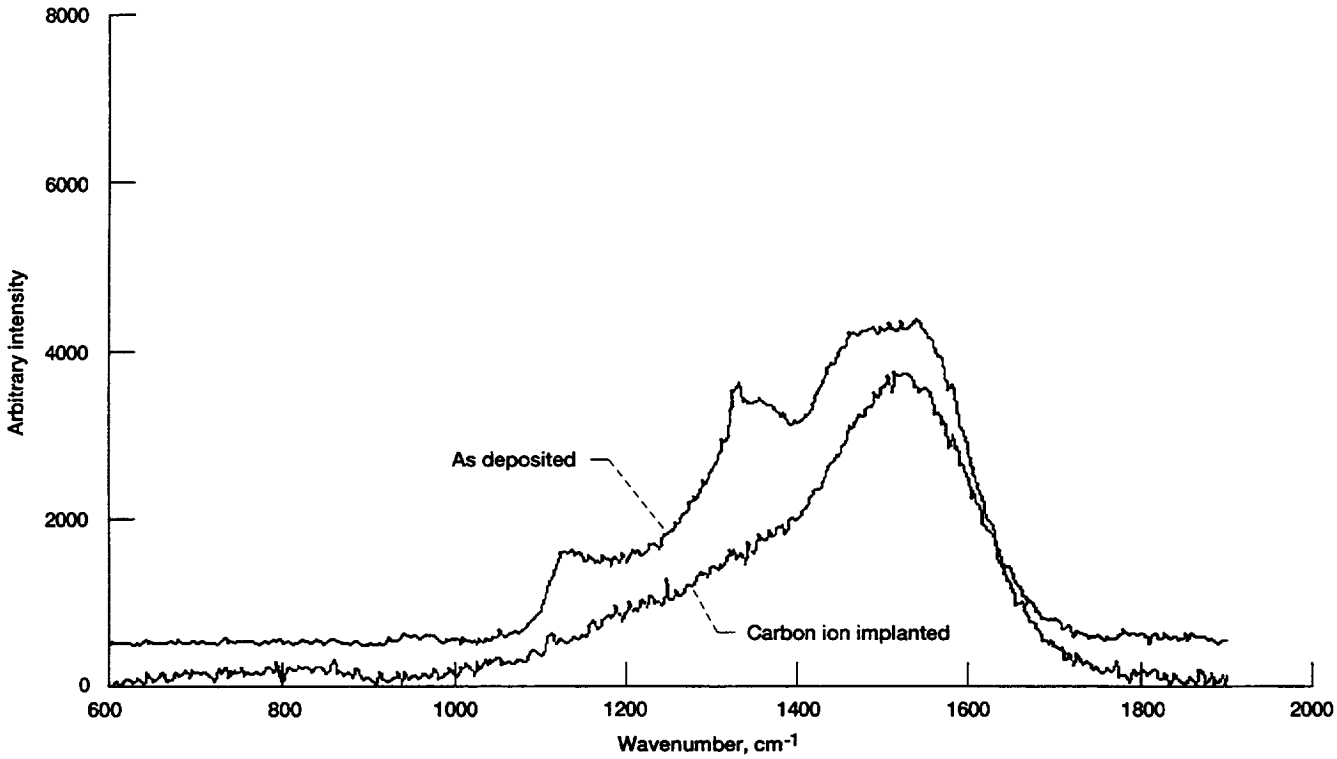

Figure 5.—Raman spectra of as-deposited and carbon-ion-implanted, fine-grain diamond film on a Si (100) substrate. Spectra are vertically displaced for viewing purposes.

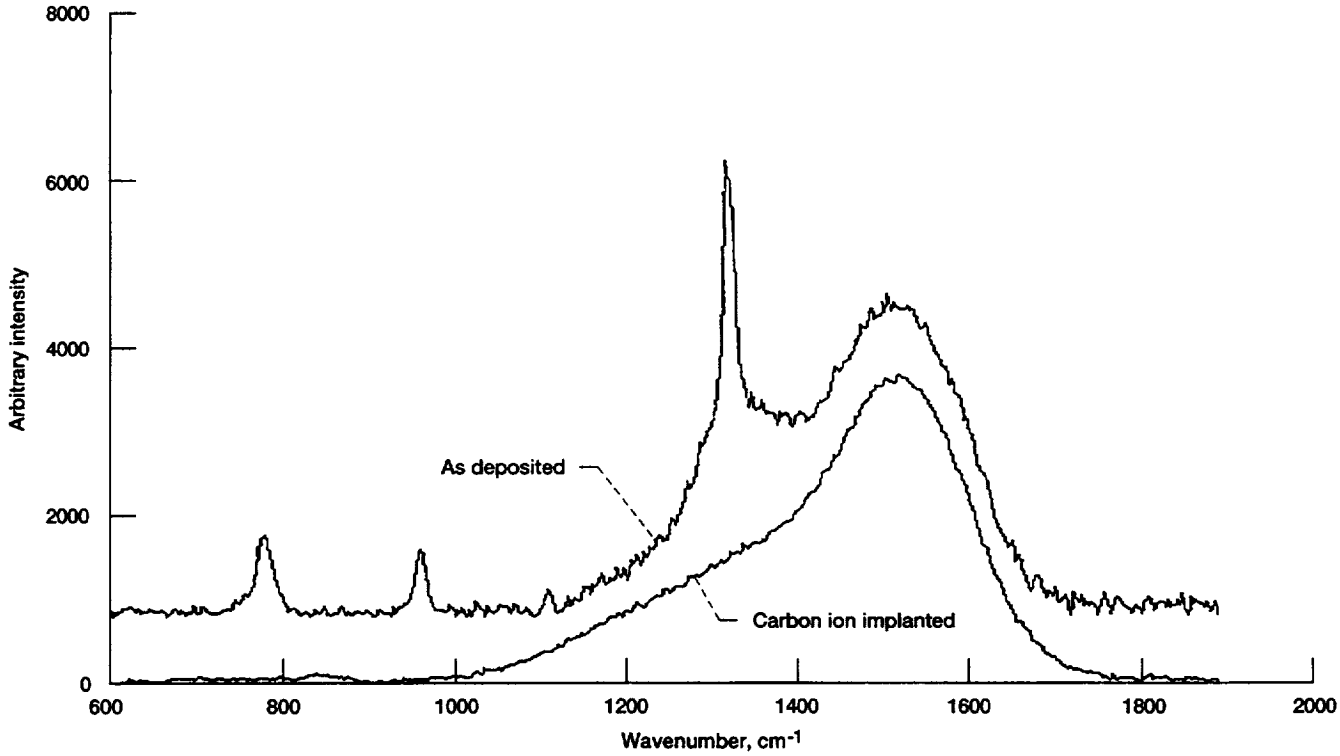

Figure 6.—Raman spectra of as-deposited and carbon-ion-implanted, coarse-grain diamond film on a Si_3N_4 substrate. Spectra are vertically displaced for viewing purposes.

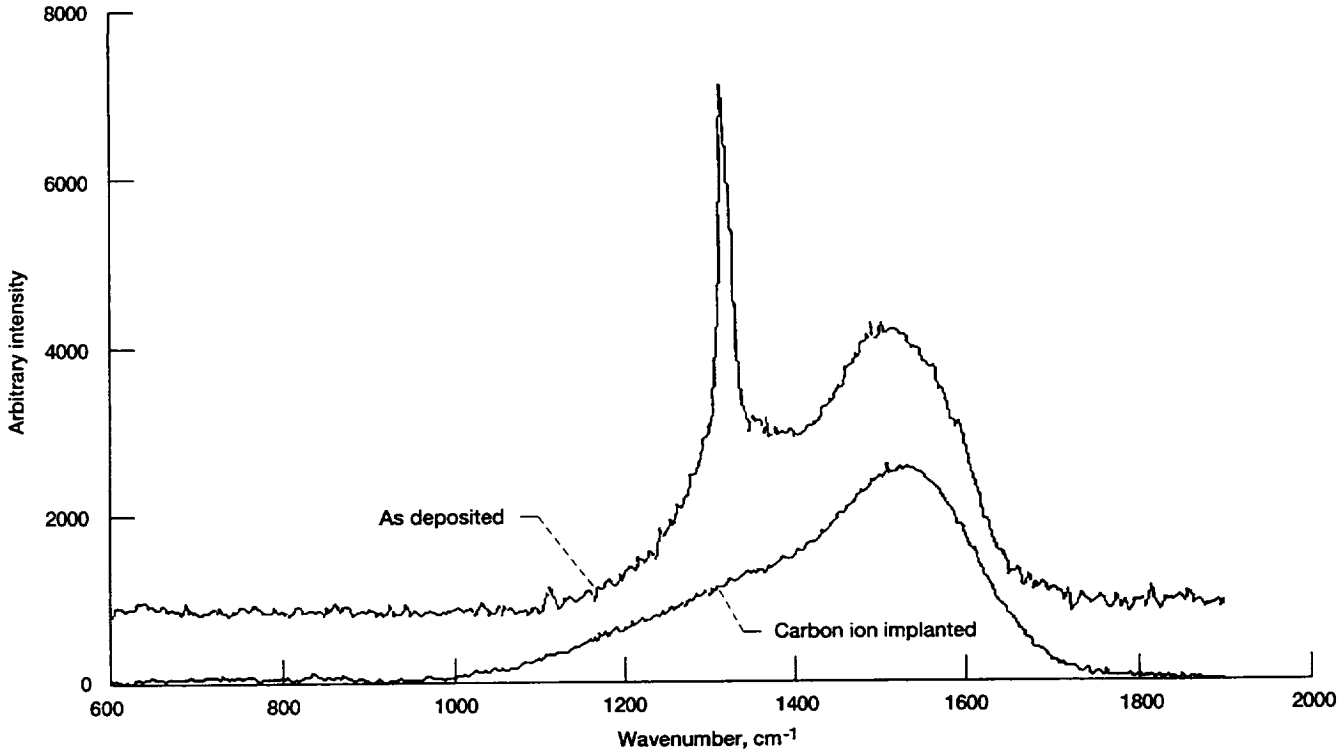

Figure 7.—Raman spectra of as-deposited and carbon-ion-implanted, coarse-grain diamond film on an α-SiC substrate. Spectra are vertically displaced for viewing purposes.

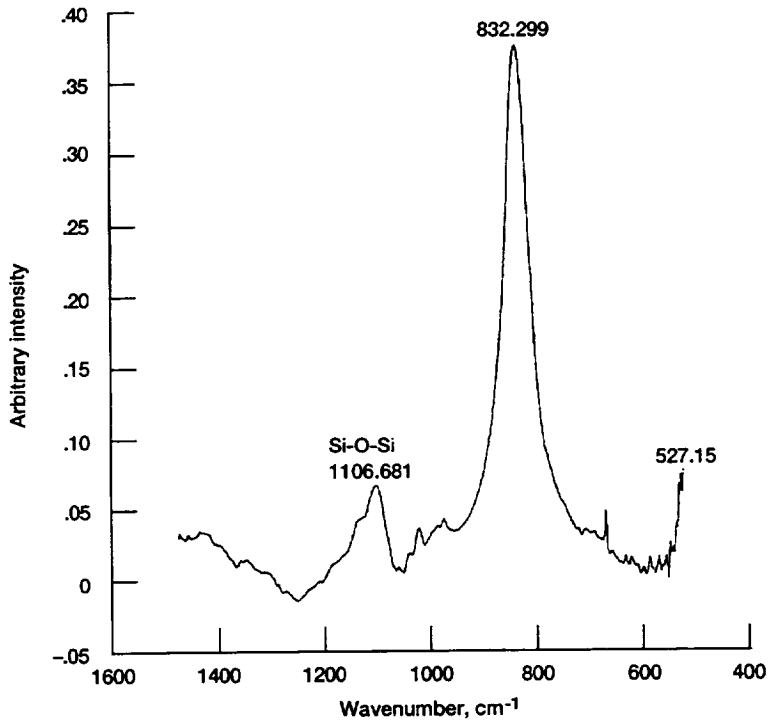

Figure 8.—Resulting Fourier transform infrared spectroscopy (FTIR) absorbance spectrum of a carbon-ion-implanted, coarse-grain diamond film after subtraction of the as-deposited film spectrum.

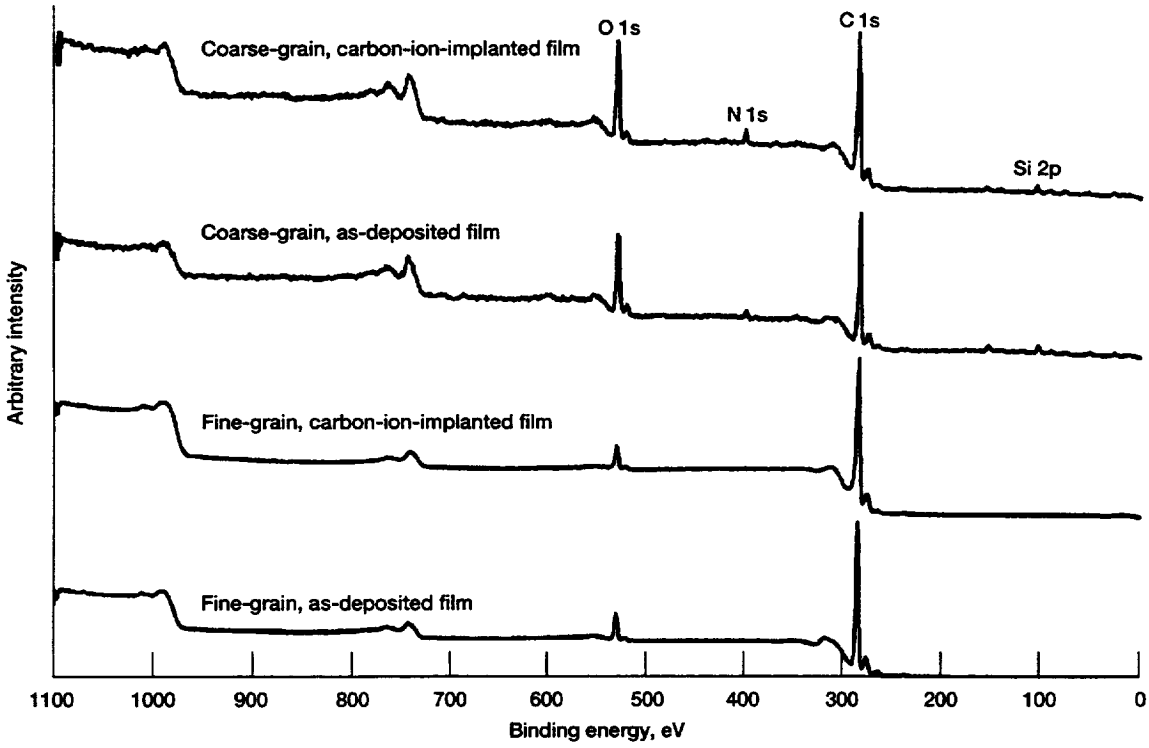

Figure 9.—X-ray photoelectron spectra of coarse- and fine-grain diamond films before and after carbon ion implantation.

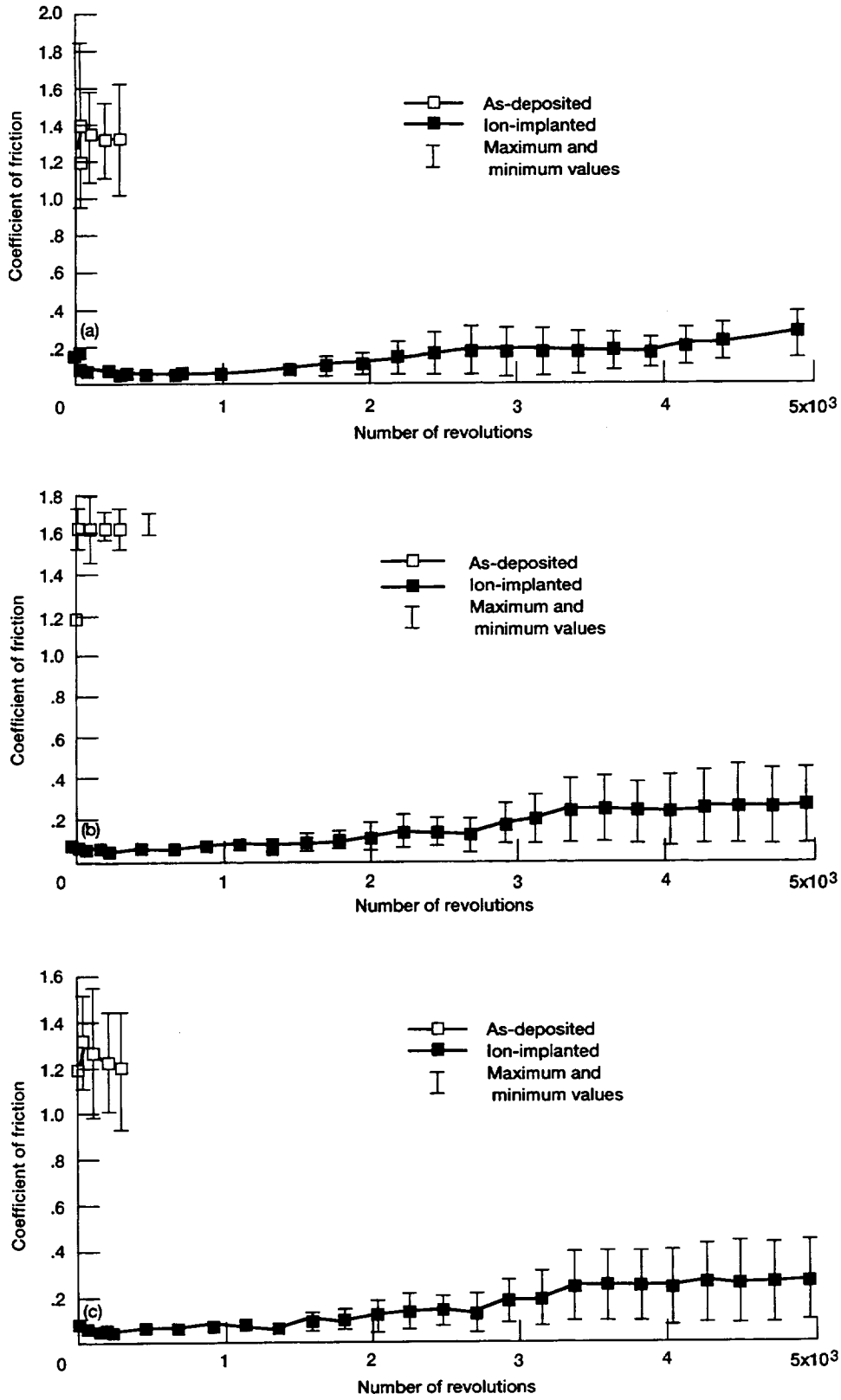

Figure 10.—Coefficient of friction of as-deposited and carbon-ion-implanted, fine-grain diamond films on Si, SiC, and Si_3N_4 substrates as functions of the number of revolutions in vacuum. (a) Si substrate. (b) SiC substrate. (c) Si_3N_4 substrate.

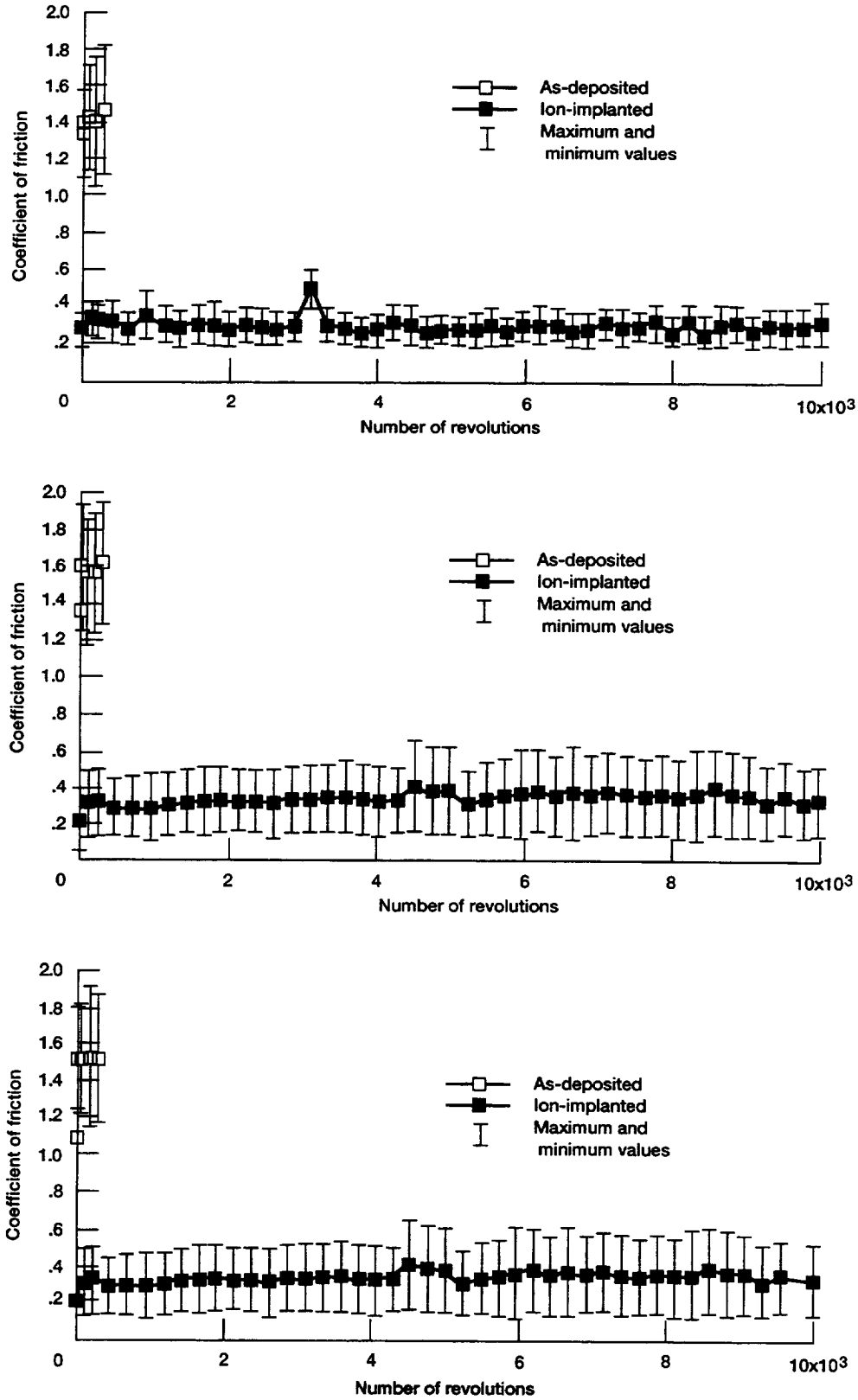

Figure 11.—Coefficient of friction of as-deposited and carbon-ion-implanted, coarse-grain diamond films on Si, SiC, and Si_3N_4 substrates as functions of the number of revolutions in vacuum. (a) Si substrate. (b) SiC substrate. (c) Si_3N_4 substrate.

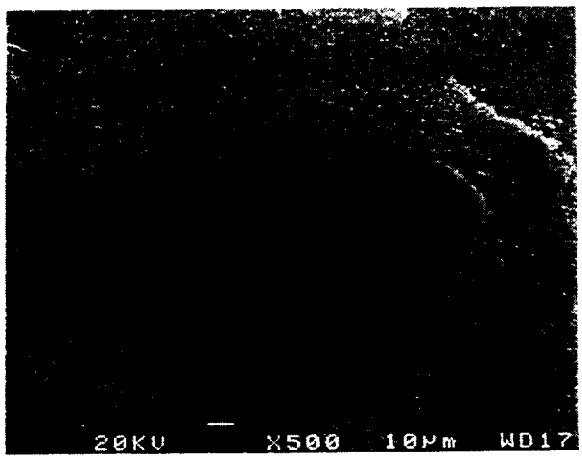

Figure 12.—Wear scar produced on diamond pin and wear track produced on fine-grain diamond film after sliding contact in vacuum. (a) SEM image of a wear scar and its surroundings. (b) SEM image of a wear track and its surroundings. (c) Profilometer record of a wear track.

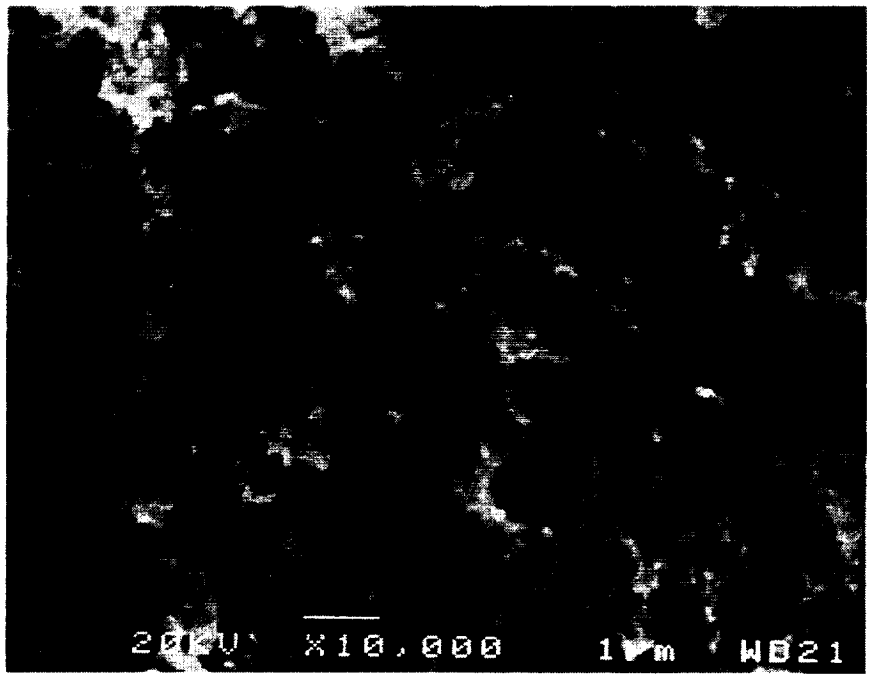

(a)

1 µm

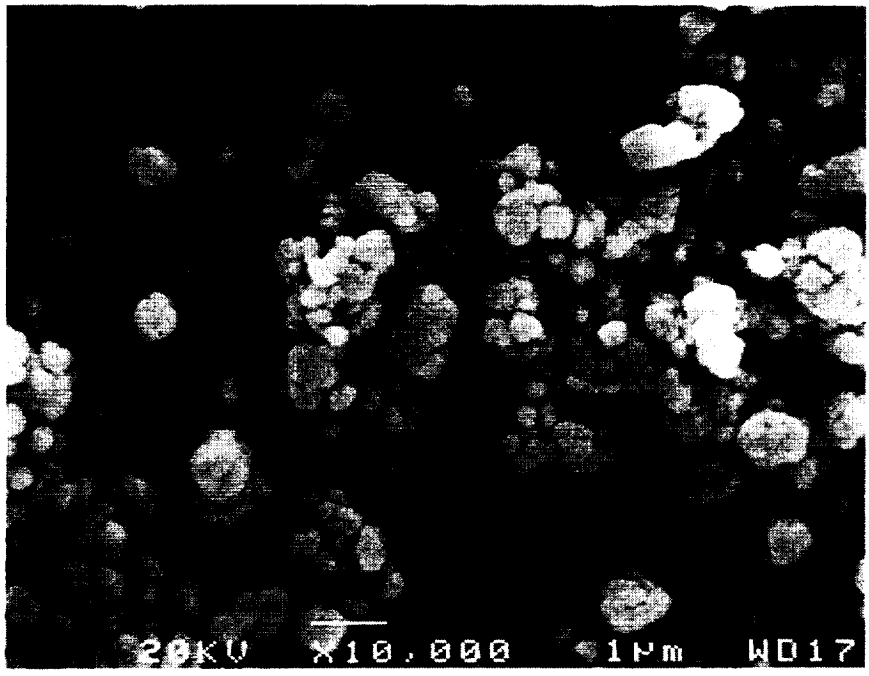

(b)

1 µm

Figure 13.—Scanning electron micrographs of a wear track and its surroundings produced on an as-deposited, fine-grain diamond film after sliding against a diamond pin in vacuum. (a) View at center of wear track on as-deposited diamond film. (b) View on side of wear track on as-deposited diamond film.

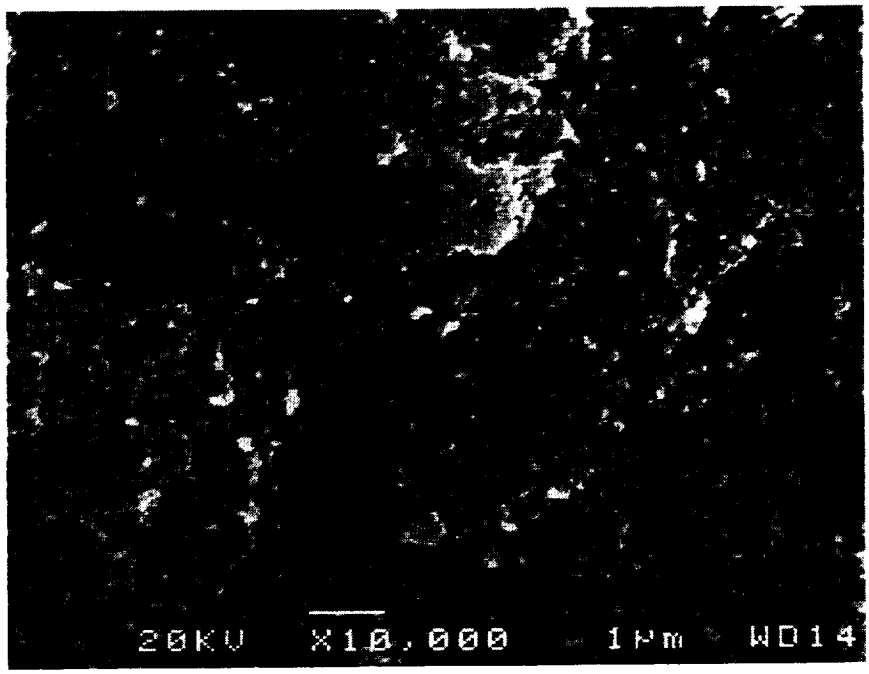

(a)

1 μm

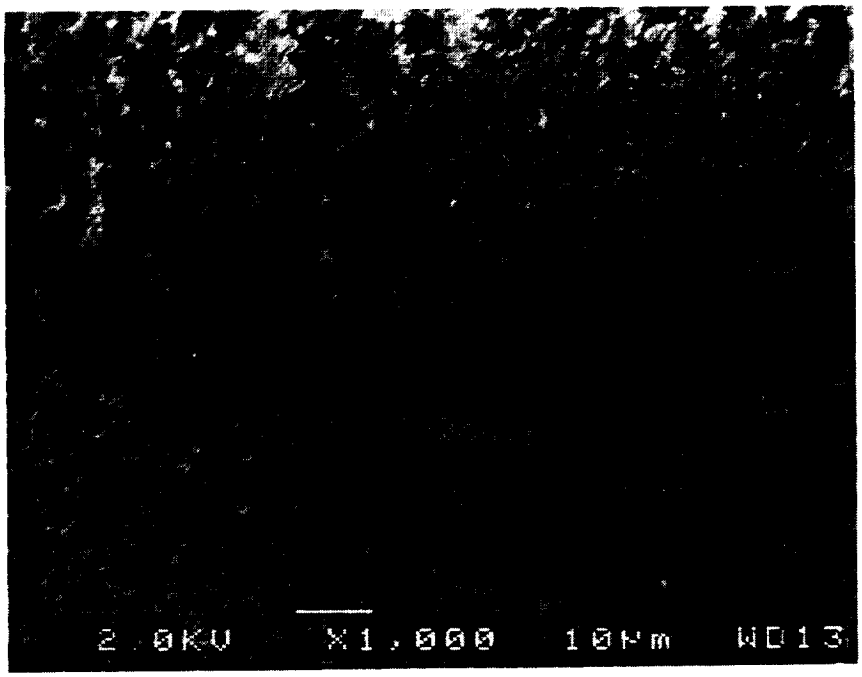

(b)

10 μm

Figure 14.—Scanning electron micrographs of a wear track and its surroundings produced on a carbon-ion-implanted, fine-grain diamond film after sliding against a diamond pin in vacuum. (a) View at center of wear track on carbon-ion-implanted diamond film. (b) View on side of wear track on carbon-ion-implanted diamond film.

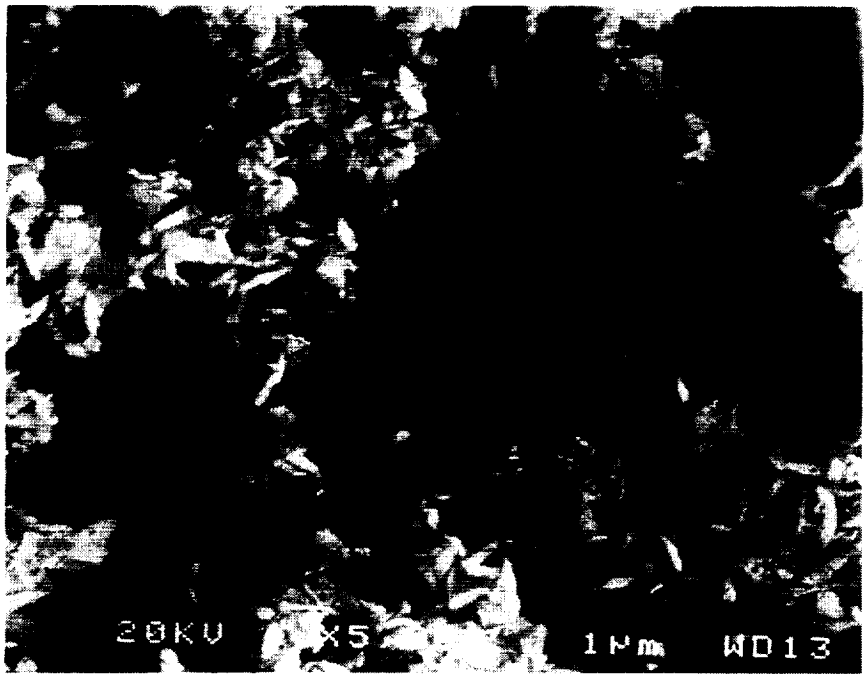

(a) 1 μm

(b) 1 μm

Figure 15.—Scanning electron micrographs of wear tracks produced on as-deposited, coarse-grain diamond films deposited on SiC substrates after sliding against a diamond pin in vacuum. (a) 1500-nm grain size. (b) 3300-nm grain size.

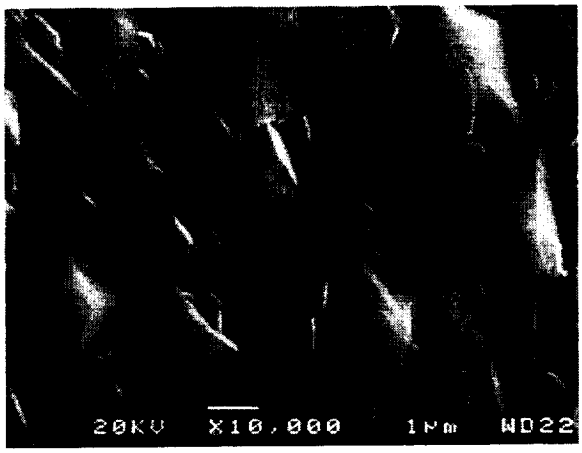

(a) 1 μm

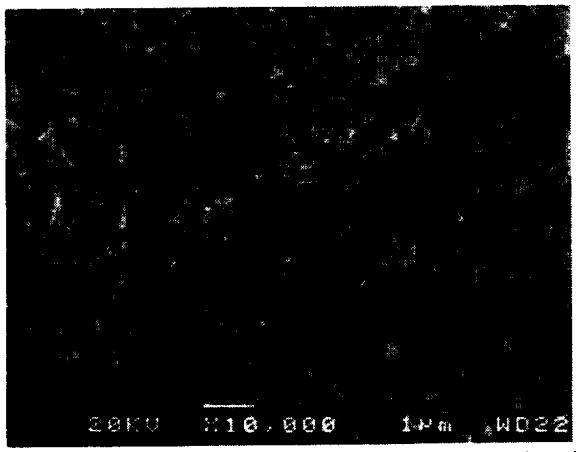

(b) 1 μm

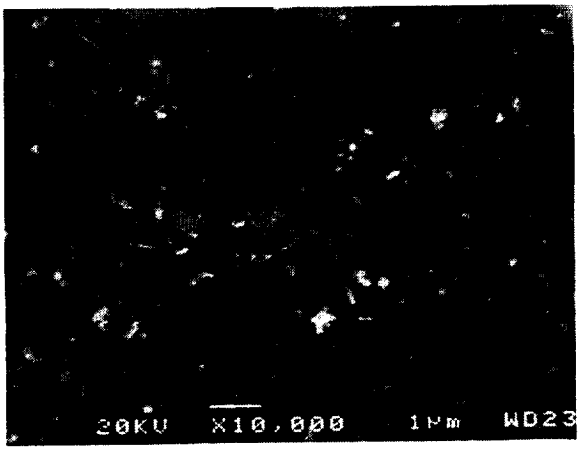

(c) 1 μm

Figure 16.—Scanning electron micrographs of a wear track and its surroundings produced on carbon-ion-implanted, coarse-grain diamond film after sliding against a diamond pin in vacuum. (a) View of carbon-ion-implanted surface. (b) View at center of wear track. (c) View on side of wear track.

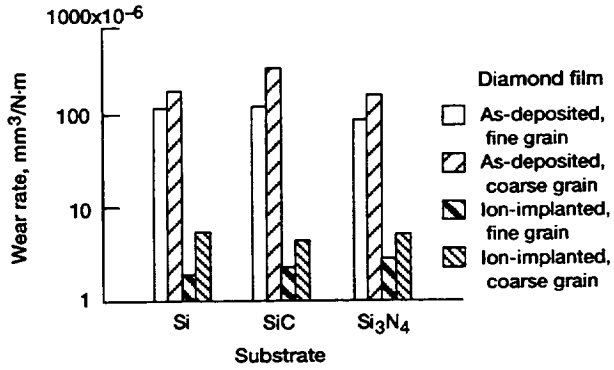

Figure 17.—Wear rates ($mm^3/N \cdot m$) of as-deposited and carbon-ion-implanted, fine- and coarse-grain diamond films on Si, SiC, and Si_3N_4 substrates sliding against a diamond pin in vacuum.

REPORT DOCUMENTATION PAGE

Form Approved
OMB No. 0704-0188

1. AGENCY USE ONLY (*Leave blank*)	2. REPORT DATE	3. REPORT TYPE AND DATES COVERED
	November 1994	Technical Memorandum

4. TITLE AND SUBTITLE

Physical and Tribological Characteristics of Ion-Implanted Diamond Films

5. FUNDING NUMBERS

WU-505-63-5A

6. AUTHOR(S)

K. Miyoshi, S. Heidger, A.L. Korenyi-Both, D.T. Jayne, P. Herrera-Fierro, B. Shogrin, P.J. Wilbur, R.L.C. Wu, A. Garscadden, and P.N. Barnes

7. PERFORMING ORGANIZATION NAME(S) AND ADDRESS(ES)

National Aeronautics and Space Administration
Lewis Research Center
Cleveland, Ohio 44135-3191

8. PERFORMING ORGANIZATION REPORT NUMBER

E-9146

9. SPONSORING/MONITORING AGENCY NAME(S) AND ADDRESS(ES)

National Aeronautics and Space Administration
Washington, D.C. 20546-0001

10. SPONSORING/MONITORING AGENCY REPORT NUMBER

NASA TM-106682

11. SUPPLEMENTARY NOTES

K. Miyoshi and S. Heidger, NASA Lewis Research Center; A.L. Korenyi-Both, Calspan Corporation, 21765 Brookpark Road, Fairview Park, Ohio 44126 (work funded by NASA Contract NAS3-25685); D.T. Jayne, P. Herrera-Fierro, and B. Shogrin, Case Western Reserve University, Cleveland, Ohio 44106; P.J. Wilbur, Colorado State University, Fort Collins, Colorado 80523; R.L.C. Wu, UES, Inc., 4401 Dayton-Xenia Rd., Dayton, Ohio 45432; A. Garscadden, and P.N. Barnes, Wright Laboratory, Wright-Patterson Air Force Base, Dayton, Ohio 45433. Responsible person, K. Miyoshi, organization code 5140, (216) 433-6078.

12a. DISTRIBUTION/AVAILABILITY STATEMENT

Unclassified - Unlimited
Subject Category 27

12b. DISTRIBUTION CODE

13. ABSTRACT ***(Maximum 200 words)***

Unidirectional sliding friction experiments were conducted with a natural, polished diamond pin in contact with both as-deposited and carbon-ion-implanted diamond films in ultrahigh vacuum. Diamond films were deposited on silicon, silicon carbide, and silicon nitride by microwave-plasma-assisted chemical vapor deposition. The as-deposited diamond films were impacted with carbon ions at an accelerating energy of 60 keV and a current density of 50 $\mu A/cm^2$ for approximately 6 min, resulting in a dose of 1.2×10^{17} carbon ions/cm^2. The results indicate that the carbon ion implantation produced a thin surface layer of amorphous, nondiamond carbon. The nondiamond carbon greatly decreased both friction and wear of the diamond films. The coefficients of friction for the carbon-ion-implanted, fine-grain diamond films were less than 0.1, factors of 20 to 30 lower than those for the as-deposited, fine-grain diamond films. The coefficients of friction for the carbon-ion-implanted, coarse-grain diamond films were approximately 0.35, a factor of 5 lower than those for the as-deposited, coarse-grain diamond films. The wear rates for the carbon-ion-implanted, diamond films were on the order of 10^{-6} mm^3/Nm, factors of 30 to 80 lower than that for the as-deposited diamond films, regardless of grain size. The friction of the carbon-ion-implanted diamond films was greatly reduced because the amorphous, nondiamond carbon, which had a low shear strength, was restricted to the surface layers (<0.1 μm thick) and because the underlying diamond materials retained their high hardness. In conclusion, the carbon-ion-implanted, fine-grain diamond films can be used effectively as wear resistant, self-lubricating coatings for ceramics, such as silicon nitride and silicon carbide, in ultrahigh vacuum.

14. SUBJECT TERMS

Friction; Wear; CVD Diamond; Vacuum

15. NUMBER OF PAGES

29

16. PRICE CODE

A03

17. SECURITY CLASSIFICATION OF REPORT	18. SECURITY CLASSIFICATION OF THIS PAGE	19. SECURITY CLASSIFICATION OF ABSTRACT	20. LIMITATION OF ABSTRACT
Unclassified	Unclassified	Unclassified	